Int J Thermophys (2010) 31:208–217
DOI 10.1007/s10765-009-0642-y

Influence of Surface Preparation for Different Groups of A2B6 Mixed Crystals

J. Zakrzewski · M. Maliński · K. Strzałkowski · F. Firszt · S. Łęgowski · H. Męczyńska

Received: 31 March 2009 / Accepted: 13 August 2009 / Published online: 29 August 2009

Abstract Piezoelectric photothermal spectroscopy has been used for measurements of the optical and thermal parameters of semiconductors. The investigated crystals were grown by the high-pressure Bridgman method under argon overpressure. The obtained photoacoustic (PA) spectra show the complexity of the effects observed for the different groups of selected A2B6 crystals. These effects comprise ideal samples and samples with damaged surfaces. The spectra show the influence of the surface treatment on the PA amplitude and phase spectra.

Keywords Mixed crystals · Piezoelectric detection · Semiconductors

1 Introduction

Photothermal methods have become a very useful tool for measurements of the optical and thermal parameters of semiconductors [1–5]. The significance of thermal phenomena becomes more and more important because of the problem of energy dissipation in miniaturized semiconducting devices. One of the thermal methods is the piezoelectric (PZE) photothermal technique, which was developed by Jackson and Amer [6] and by Blonskij et al. [7]. This method was successfully used to investigate the properties of A2B6 mixed crystals [8–10].

J. Zakrzewski (✉) · K. Strzałkowski · F. Firszt · S. Łęgowski · H. Męczyńska
Instytut Fizyki, Uniwersytet Mikołaja Kopernika, ul. Grudziądzka 5/7, 87–100 Torun, Poland
e-mail: jzakrzew@fizyka.umk.pl

M. Maliński
Department of Electronics, Technical University of Koszalin, ul. Sniadeckich 2,
75–328 Koszalin, Poland

Wide gap II–VI compounds are still the subject of intense research, mainly because of their application in bandgap engineering, interband and intersubband transitions, and dilute semiconductors, materials and devices. For these materials, it is possible to change electronic properties, lattice parameters, and bandgap energies by adjusting the composition of the mixed crystals. The change of the bandgap energy gives the desired optical properties and emission in the entire visible and uv ranges of the spectrum.

The II–VI semiconductors exhibit high polarity, which results in degradation in laser structures. $Cd_{1-x}Mn_xTe$ mixed crystals belong to a class of materials called "semimagnetic semiconductors" or "diluted magnetic semiconductors (DMS)". This term is applied to alloys in which one component is a magnetic semiconductor and the second is non-magnetic. $Cd_{1-x}Mn_xTe$ shows very interesting physical properties due to strong s, p–d exchange interactions between electrons, holes, and ion Mn^{+2}–3d electrons. Recently, beryllium chalcogenides BeSe and BeTe were proposed as constituents of the mixed wide-gap II–VI compounds. The beryllium chalcogenides BeS, BeSe, and BeTe exhibit interesting properties, e.g., BeS has very high hardness and BeTe is a p-type semiconductor of the zinc blende structure. Quaternary $Zn_{1-x-y}Be_xMn_ySe$ is particularly interesting because a partial substitution of Zn by Be allows for control of the structure (lattice constant) and the energy gap of the material.

The PZE technique is very sensitive and is considered to be a direct method as the signal depends on the quantum yield of the nonradiative transitions in semiconductors. It is also a complementary technique to absorption and photoluminescence spectroscopy. This technique, although relatively easy and convenient experimentally using a phase sensitive method, is difficult for quantitative interpretation.

The aim of this article is to present the influence of the surface preparation process on the PZE spectra of some groups of A2B6 compounds. The spectra were measured at various steps during the process of preparation for optical measurements, e.g., photoluminescence, which demands high quality surface.

2 Experimental

All the samples were grown from high purity powder with the high-pressure Bridgman method. For all materials, the crystal rods were cut into about 1 mm thick samples, which were first ground using grinding powder (diameter of 10 μm). Some of them were then polished with diamond paste (1 μm) and finally chemically etched. A solution of H_2SO_4 (96 %), $K_2Cr_2O_7$, and water was used for etching the samples. After etching, the samples were rinsed in distilled water and then put in boiling NaOH for a few seconds. Then, the samples were rinsed again in cold water and next in boiling distilled water, and finally in ethyl alcohol.

Figure 1 presents the theoretical predictions for the amplitude and phase spectra in the rear mode [8] configuration. A characteristic peak in the sub-bandgap region in the amplitude spectrum is clearly visible. According to the Jackson–Amer theory [6], the peak is due to subtracting the components coming from the piston and drum effect in the rear configuration mode [8]. In the phase spectra, this phenomenon is manifested as a change in the zero crossing energy value (when the compensation

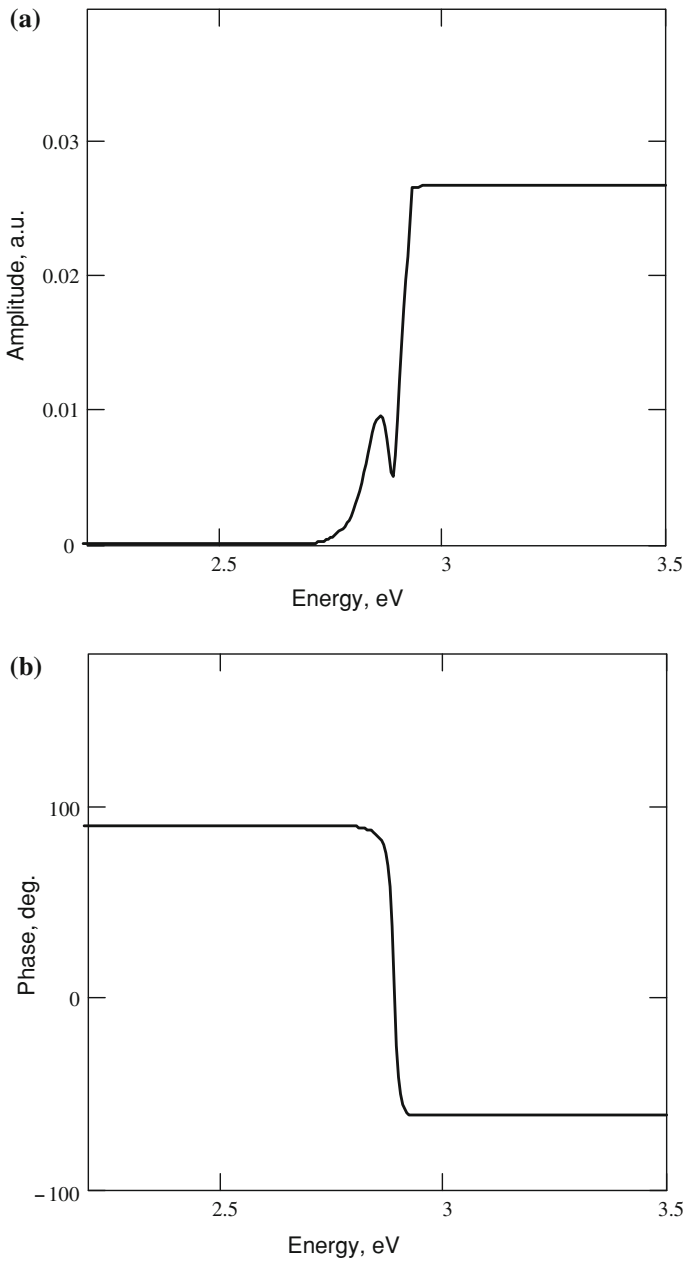

Fig. 1 Theoretical predictions for the (**a**) amplitude and (**b**) phase spectra in the rear mode configuration

for bending and expansion of the sample due to heating occurs, the PZE transducer situated behind the sample registers an amplitude signal that goes to zero at $\alpha l = 2$, where α is the absorption coefficient and l is the sample thickness). Figure 2 presents

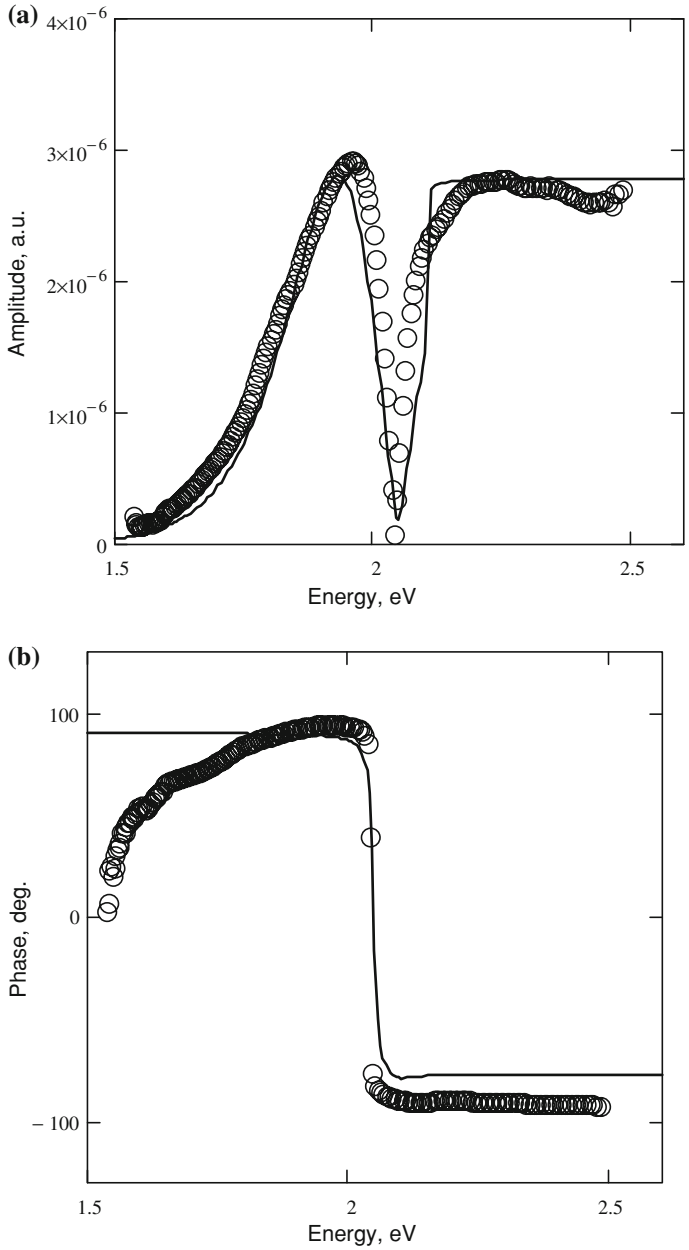

Fig. 2 Experimental (*circle*) and theoretical (*solid line*): (**a**) amplitude and (**b**) phase spectra for polished $Cd_{0.88}Mg_{0.12}Se$ mixed crystal

the experimental (circle) and theoretical (solid line) (a) amplitude and (b) phase spectra for a polished $Cd_{0.88}Mg_{0.12}Se$ mixed crystal for 16 Hz modulation frequency. All the characteristic features of the theoretical predictions are visible. The increase of

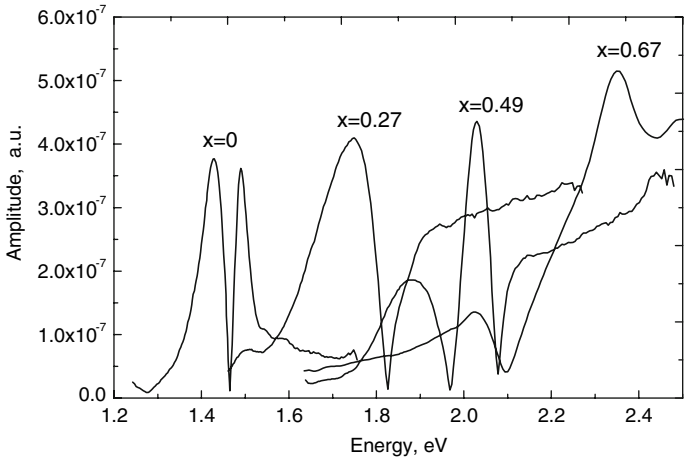

Fig. 3 Amplitude spectra of polished $Cd_{1-x}Mn_xTe$ mixed crystals for different content of Mn

modulation frequency causes the increase of the maximum in the sub-bandgap region. The computations of the PZE spectra for photon energies in the range of the main absorption band were performed for optical absorption coefficient spectra, for energies below and above the energy gap (E_g) of the crystal, described with Eqs. 1 and 2, respectively [8], as follows:

$$\beta(E) = \beta_0 \exp\left(\frac{(E-E_g)\gamma}{0.025}\right) \quad \text{for } E < E_g \tag{1}$$

$$\beta(E) = A_0 \left(E - E_g\right)^{1/2} \quad \text{for } E < E_g \tag{2}$$

Equation 1 describes Urbach tail thermal broadening of the absorption band observed for all direct electron type transition semiconductors. Equation 2 describes the absorption band connected with the direct, band-to-band, electron transitions in semiconductors. The computations were performed for the following set of parameters: $\beta_0 = 100\,\mathrm{cm}^{-1}$, $A_0 = 0.005\,\mathrm{cm}^{-1}$, $\gamma = 0.3$, and $E_g = 2.1\,\mathrm{eV}$.

Figure 3 presents amplitude spectra of polished $Cd_{1-x}Mn_xTe$ mixed crystals for different content of Mn. The different content of Mn changes the values of the energy gap, which shift to higher values with increasing manganese content, x. For the case of $x = 0.49$, the additional maximum at a energy of 2.03 eV is observed. Figure 4 shows the comparison of amplitude and phase spectra for two different contents of Mn, (a) 0.27 and (b) 0.49. In the first case, the near ideal character of the amplitude and phase spectrum measured in the rear configuration of the polished sample is observed. However, an interesting change almost of the value of the energy gap is observed in the phase spectra in (a), indicated by the arrows. This bending is associated with additional sources of heat associated with surface defects [8], the effect of which is too small (or it is compensated) to be observed in the amplitude. As is shown in [8], the effects visible in the phase spectra cannot be observed in the amplitude spectra. The different character of the amplitude and phase is observed for the case of

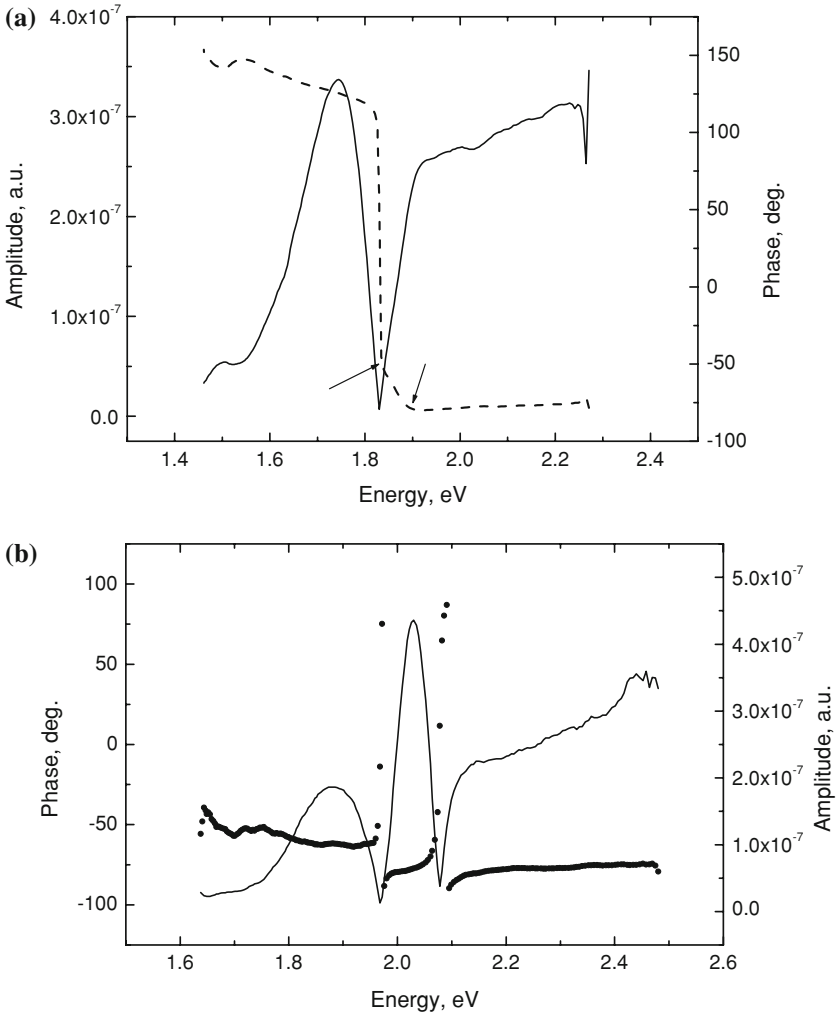

Fig. 4 Amplitude (*solid*) and phase (*dash*) spectra for (**a**) $Cd_{0.73}Mn_{0.27}Te$ and (**b**) $Cd_{0.51}Mn_{0.49}Te$

$x = 0.49$. The maximum (2.03 eV) in the sub-bandgap region of the amplitude spectra dominates. It is also associated with the changes (the step between 1.98 eV and 2.06 eV) in the phase spectrum. All the samples were prepared in the same way: cut and polished. The origin of the peak at 2.027 eV is unknown, and it can be explained if one compares the spectra of $Zn_{0.9}Be_{0.05}Mn_{0.05}Se$ for different ways of surface preparation. Figure 5 shows amplitude and phase spectra for three types of preparation for $Zn_{0.9}Be_{0.05}Mn_{0.05}Se$ samples: etched, polished, and ground. The phase spectra show three types of its behavior. Although at first sight they exhibit different behavior, the changes (bending points) occur in the same energy values and they are equivalent. From the point of theoretical predictions, the correct shape is for the etched sample [8]. In character, the amplitude spectra are very similar to the spectra of $Cd_{0.51}Mn_{0.49}Te$

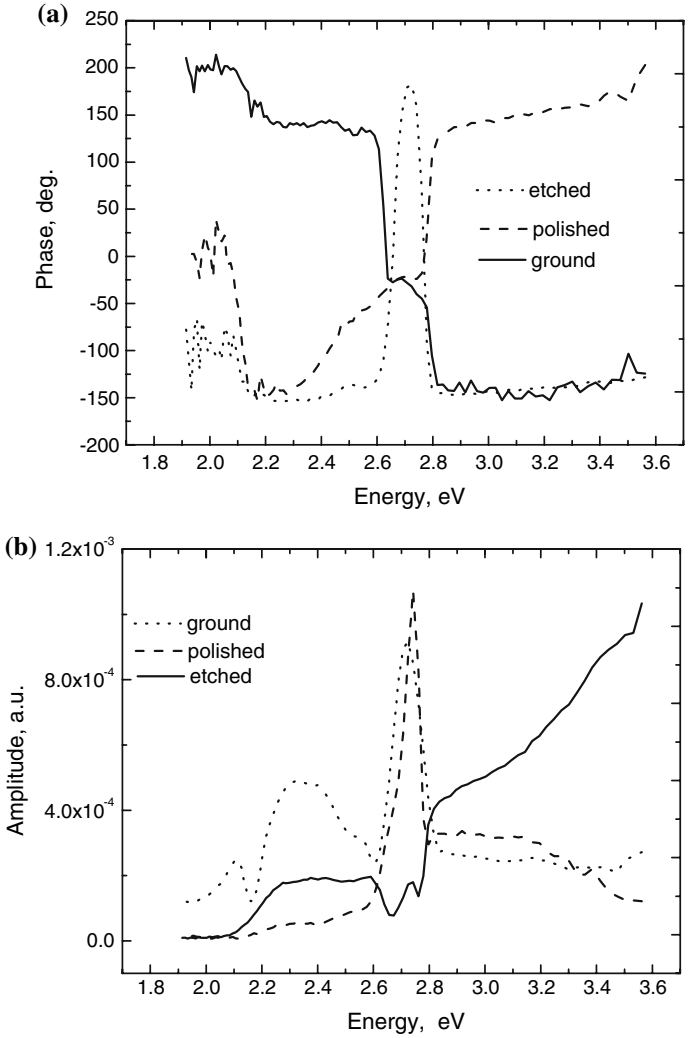

Fig. 5 (**a**) Amplitude and (**b**) phase spectra for three types of preparation for $Zn_{0.9}Be_{0.05}Mn_{0.05}Se$ samples: etched, polished, and ground

with the additional maximum at the energy bandgap value. The better is the quality of the surface—after polishing and etching, the lower is the value of the maximum in the amplitude spectra.

Hence, one can state that these sub-bandgap peaks are associated with the surface states, which arose during the surface treatment process. The confirmation and theory of this phenomena for the $Zn_{0.9}Be_{0.05}Mn_{0.05}Se$ were published in [8].

In the interpretation of the PA signal, one must consider periodical temperature fields generated in the sample caused by the absorption of the intensity modulated periodical optical radiation. In the interpretation of the obtained signals, volume and

surface absorptions must be taken into account. They are associated with the volume absorption type temperature distribution T_V and one of the temperature distributions connected with the surface absorption on one of the surfaces of the sample T_{SL} or T_{SR}. Defects located at different surfaces exert different types of influence on the photoacoustic signal. The temperature distribution in the sample can be expressed by the following equations depending on the location of the surface defects:

$$T_L(x,\beta) = T_{SL}(x,\beta,\alpha,f,l,d) + T_V(x,\beta,\alpha,f,l) \tag{3}$$

$$T_R(x,\beta) = T_{SR}(x,\beta,\alpha,f,l,d) + T_V(x,\beta,\alpha,f,l) \tag{4}$$

$$T_{SL}(x,\beta) = \frac{I_0\left(1-\exp(-\beta d)\right)\left(\exp(-\sigma x)+\exp(-2\sigma l+\sigma x)\right)}{\lambda\sigma\left(1-\exp(-2\sigma l)\right)} \tag{5}$$

$$T_{SR}(x,\beta) = \frac{I_0\left(1-\exp(-\beta d)\right)\left(\exp(-\sigma(l-x))+\exp(-2\sigma l+\sigma(l-x)\right)}{\lambda\sigma\left(1-\exp(-2\sigma l)\right)} \tag{6}$$

$$T_V(x,\beta) = \frac{\beta I_0\left(M(x,\beta)+N(x,\beta)\right)}{2\lambda\sigma\left(1-\exp(-2\sigma l)\right)} \tag{7}$$

$$M(x,\beta) = \frac{\exp(-\sigma x)-\exp(-\beta x)+\exp(-\sigma(2l-x))}{\beta-\sigma} - \frac{-\exp(-\sigma l+\sigma x-\beta l)+\exp(-2\sigma l-\beta x)-\exp(-\sigma l-\sigma x-\beta l)}{\beta-\sigma}$$

$$N(x,\beta) = \frac{\exp(-\sigma x)+\exp(-2\sigma l+\sigma x)-\exp(-2\sigma l-\beta x)}{\beta+\sigma} + \frac{\exp(-\beta x)-\exp(-(\sigma+\beta)l+\sigma x)-\exp(-\sigma x-\sigma l-\beta l)}{\beta+\sigma}$$

$$0 \le x \le l$$

where $T_{SL}$is the temperature distribution associated with the surface defects located on the illuminated side of the sample, T_{SR} is the analogous distribution but associated with the defects located on the opposite side of the sample, T_V is the temperature distribution associated with the volume absorption of light in the sample, x is the spatial coordinate, β is the optical absorption coefficient, α is the thermal diffusivity of the sample, l is the thickness of the sample, d is the thickness of the surface defect layer, and f is the frequency of modulation. The PZE signal S is expressed by

$$S_{L/R} \cong -\left(\frac{1}{l}\int_0^l T_{L/R}(x,\beta)\,dx - \frac{6}{l^2}\int_0^l \left(\frac{l}{2}-x\right) T_{L/R}(x,\beta)\,dx\right) \tag{8}$$

The surface states can be easily observed for $Zn_{0.9}Be_{0.05}Mn_{0.05}Se$ mixed crystals. They were also observed for the case of $Cd_{1-x}Mn_xTe$ for the sample, the surface of which was not ideal. To confirm that photoacoustic PZE spectroscopy can be used as the tool for surface defect measurements, ground and polished samples of $Cd_{0.6}Zn_{0.2}Mg_{0.2}Se$ were measured. Figure 6 shows experimental (circles) and theoretical (solid line) amplitude and phase spectra for ground (a,b) and polished

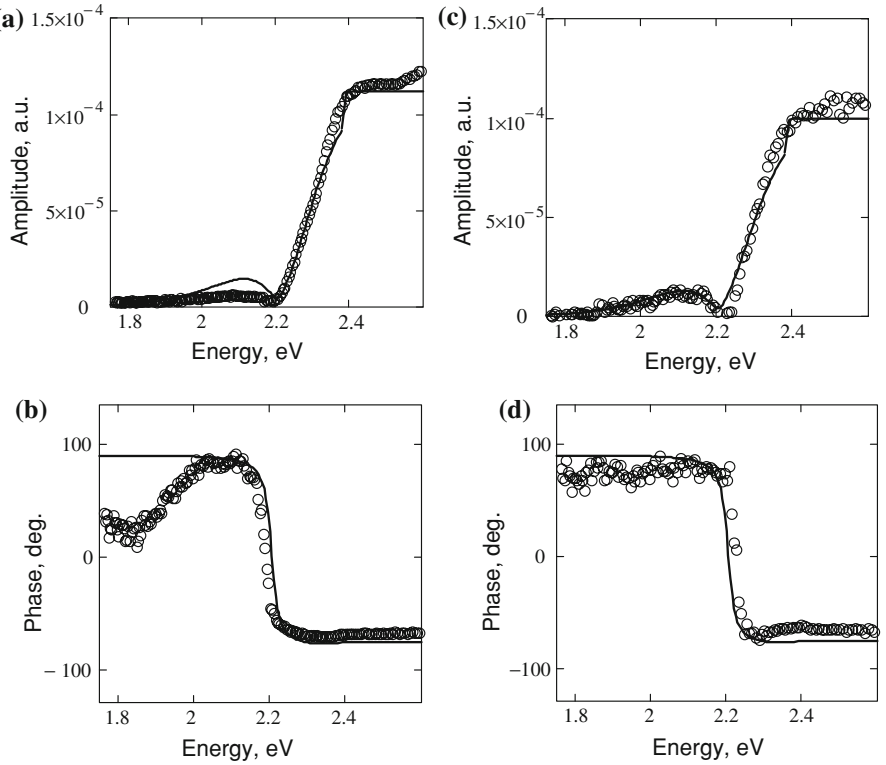

Fig. 6 Experimental (*circles*) and theoretical (*solid line*) amplitude and phase spectra for (**a**), (**b**) ground and (**c**), (**d**) polished $Cd_{0.6}Zn_{0.2}Mg_{0.2}Se$ samples

samples (c,d). The fitting procedure was the same as for the data presented in Fig. 2, with the values of parameters as follows: $\beta_0 = 200\,\mathrm{cm}^{-1}$, $A_0 = 0.005\ \mathrm{cm}^{-1}$, $\gamma = 0.3$, and $E_g = 2.38\,\mathrm{eV}$. No maximum or characteristic changes in the phase spectra are observed for either sample, the results of the fact that the surface states are located on both sides of the samples. The polished samples exhibit a smaller density of surface states, in the range of energies from 1.8 eV to 2.2 eV, compared to the ground sample.

3 Conclusions

The PA spectra presented in the article show the complexity of the effects observed for mixed crystals of selected $A^{II}B^{VI}$ compounds. These effects comprise ideal samples and also samples with damaged surfaces. They are observed mainly as sub-bandgaps of the crystals. The spectra also show the influence of the surface treatment on the PA amplitude and phase spectra. The spectra are the subject of numerical modeling in a two-layer model of the sample presented previously [8–10]. This model enables computations of the influence of the surface states on the photoacoustic spectra of mixed crystals. Observed effects depend on the crystal lattice structure. Strong surface effects

can be seen for crystals of the sphalerite structure (ZnBeMnSe, CdMnTe), whereas for those of the wurzite structure (CdMgSe, CdZnMgSe), these effects are not clearly pronounced. More detailed investigations to confirm this statement are in progress.

References

1. P. Wang, T. Nakagawa, A. Fukuyama, K. Maeda, Y. Iwasa, M. Ozeki, Y. Akashi, T. Ikari, Mater. Sci. Eng. C **26**, 826 (2006)
2. A. Fukuyama, S. Sakamoto, S. Sonoda, P. Wang, K. Sakai, T. Ikari, Thin Solid Films **112**, 511 (2006)
3. K. Sakai, T. Kakeno, T. Ikari, S. Shirakata, T. Sakemi, K. Awai, T. Yamamoto, J. Appl. Phys. **99**, 043508 (2006)
4. K. Yoshino, H. Komaki, T. Kakeno, Y. Akaki, T. Ikari, J. Phys Chem. Solids **64**, 1839 (2003)
5. S. Sato, A. Memon, A. Fukoyama, S. Tanaka, T. Ikari, Rev. Sci. Instrum. **74**, 340 (2003)
6. W. Jackson, N.M. Amer, J. Appl. Phys. **51**, 3343 (1980)
7. I.V. Blonskij, V.A. Thoryk, M.L. Shendeleva, J. Appl. Phys. **79**, 3512 (1996)
8. M. Maliński, J. Zakrzewski, K. Strzałkowski, Int. J. Thermophys. **28**, 299 (2007)
9. M. Maliński, J. Zakrzewski, K. Strzałkowski, S. Łęgowski, F. Firszt, H. Męfczyńska, Surf. Sci. **603**, 131 (2009)
10. M. Maliński, J. Zakrzewski, F. Firszt, Eur. Phys. J. Special Top. **153**, 251 (2008)